EDM2001,BNL
05/14/01

MUON g-2 IN SUGRA MODELS

R. Arnowitt

B. Dutta

B. Hu

Y. Santoso

Ref: hep-ph/0102344 Texas A&M University

1. INTRODUCTION

Over the past 25 years the muon's anomalous magnetic moment

$$a_\mu \equiv \frac{1}{2}(g_\mu - 2)$$

has been measured with increasing accuracy. With the latest BNL data, one has the average

$$a_\mu^{EXP} = 116\,592\,023(151) \times 10^{-11}$$

[Czarnecki, Marciano]

One of the motivations of the BNL experiment was to test the Standard Model, and particularly the electroweak contribution:

$$a_\mu^{EW} = 152(4) \times 10^{-11}$$

and current data is at the edge of doing this.

However, there already appears to be a possible 2.6σ deviation from the expected Standard Model result

$$a_\mu^{EXP} - a_\mu^{SM} = 43(16) \times 10^{-10}$$

[Brown etal, hep-ex/0102017]

A recent re-evaluation of the hadronic contribution to a_μ^{SM} by Narison gave a similar result

$a_\mu^{EXP} - a_\mu^{SM} = 38(17) \times 10^{-10}$ [hep – ph/0103199]

(See also Marciano, Roberts, hep-ph/0105056)

These results suggest the presence of new physics. There are many possibilities. Supersymmetry offers a natural explanation for a deviation of a_μ^{EXP} from a_μ^{SM}, and we consider that here.

2. SUPERSYMMETRY

In supersymmetry there are the following particles which contribute to a_μ:
$\tilde{\chi}_i^\pm$, $i = 1, 2$, chargino;
$\tilde{\chi}_k^0$, $k = 1...4$, neutralinos
$\tilde{\mu}_i$; i=1,2, smuons
$\tilde{\nu}$; sneutrino
and they contribute to a_μ from the diagrams

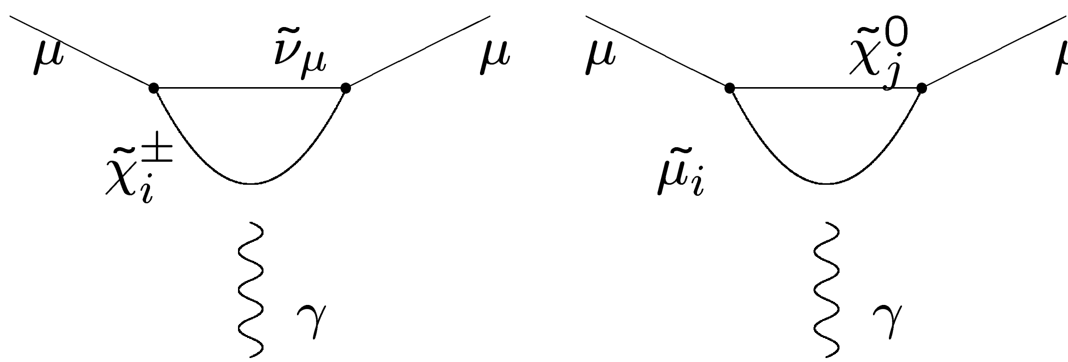

along with the Standard model diagrams

Global Supersymmetry

The initial calculations are done within the framework of global supersymmetry, 1980-1982 [Fayet, Grifols, Mendez, Ellis, Hagelin, Nanopoulos, Barbieri, Maianai].

However there exists a theorem that says for unbroken global supersymmetry

$$a_\mu = 0 \text{ [Ferrara, Remiddi, 1974]}$$

One needs broken supersymmetrey to get a non-zero result, and a phenomenologically satisfactory way of breaking global supersymmetry did not exist.

Supergravity(SUGRA) Models

In local supersymmetry (supergravity) spontaneous breaking of SUSY occurs naturally and the first calculation of a_μ^{SUGRA} using SUGRA GUT models done were:

Kosower, Kraus, Sakai [1983]

Yuan, Arnowitt, Chamseddine, Nath [1984] (first complete calculation)

Here SUSY breaking triggers electroweak breaking so that

$$M_{\text{SUSY}} \simeq M_{\text{Electroweak}} \simeq < H > (246\text{GeV})$$

This sets scale of SUSY masses to be

$$\simeq 100\text{GeV} - 1\text{TeV}$$

and determines scale of a_μ^{SUGRA}.

This mass scale is supported by the following:

(i) LEP data is consistent with grand unification at $M_G \simeq 2 \times 10^{16}$ GeV if SUSY masses lie $\simeq$ 100 GeV-1 TeV [1990].

(ii) SUGRA models with R-parity invariance have dark matter candidate, the lightest neutralino, $\tilde{\chi}_1^0$, with astronomically observed amount of relic density when SUSY masses $\simeq$ 100 GeV-1 TeV [1983].

We have considered a_μ^{SUGRA} for following SUGRA GUT models with R-parity invariance:

(i) Models with universal soft breaking at M_G (mSUGRA).

(ii) Models with non-universal soft breaking scalar masses at M_G in Higgs and 3rd generation squarks and sleptons.

(iii) Models with CP violating phases in soft breaking parameters at M_G-relate a_μ to electric dipole moments (EDMs).

Consider in this talk (i) and (ii) and (iii) will be discussed in Bhaskar Dutta's talk.

SUGRA models apply to wide range of phenomena; accelerator physics, dark matter (cosmology), a_μ. Information in one area influences predictions in another, and one needs to fit all data simultaneously to get the predictions of a model.

We use following constraints:

(i) Accelerator bounds:

$m_h > 114$ GeV (LEP bound)

$m_h > 120$ GeV

$b \to s\gamma$ bounds:

$1.8 \times 10^{-4} < BR(b \to s\gamma) < 4.5 \times 10^{-4}$

Tevatron and LEP SUSY mass bounds

(ii) Relic density bounds:

$$0.025 \leq \Omega_{\tilde{\chi}_1^0} h^2 \leq 0.25$$

(iii)a_μ^{SUGRA} 2σ bounds of BNL experiment:

$$11 \times 10^{-10} \leq a_\mu^{\mathrm{SUGRA}} \leq 75 \times 10^{-10}$$

3. TECHNICAL DETAILS

In order to get accurate results, need to include a number of corrections:

(i) Relic density calculations
coannihilation $\tilde{\tau}_1 - \tilde{\chi}^0_1$ effects
large $\tan\beta$
[Arnowitt, Dutta, Santoso, hep-ph/0102181, Ellis etal hep-ph/0102098]

(ii) Large $\tan\beta$ NLO corrections to $b \to s\gamma$ decay [Degrassi etal., Carena etal.]

(iii) Loop corrections to m_b, m_τ (important for large $\tan\beta$)

(iv) Two loop and pole mass corrections to m_h

Note: there still exists theoretical uncertainty in $m_h \simeq 3$ GeV and so assume here conservatively that theory overestimates

Do not assume Yukawa unification or proton decay as these depend on unknown physics beyond M_G.

4. mSUGRA MODEL

mSUGRA model depends on 4 parameters and 1 sign:

m_0: Scalar soft breaking mass at M_G

$m_{1/2}$: Gaugino mass at M_G ($m_{\tilde{\chi}_1^0} \simeq 0.4 m_{1/2}$; $m_{\tilde{\chi}_1^\pm} \simeq 0.8 m_{1/2}$)

A_0: cubic soft breaking mass at M_G

tanβ: $< H_2 > / < H_1 >$ at the electroweak scale

$\frac{|\mu|}{\mu}$: sign of Higgs mixing parameter ($W^{(2)} = \mu H_1 H_2$)

Parameter range:
m_0, $m_{1/2} \leq 1$ TeV ($M_{\tilde{g}} \leq 2.5$ TeV)
$2 \leq \tan\beta \leq 40$
$|A_0| \leq 4m_{1/2}$

We consider now the consequences of this model [Arnowitt, Dutta, Hu, Santoso, hep-ph/0102344, see also Ellis, Nanopoulos, Olive, hep-ph/0102331].

It is well known that a_μ^{SUGRA} increases with $\tan\beta$[Kosower etal. 1983] and we will see that the data favors large $\tan\beta$. For large $\tan\beta$ the chargino diagrams dominate, and for $M_W^2/\mu^2 << 1$ one finds

$$a_\mu^{\tilde{\chi}^\pm} \simeq \frac{\alpha}{4\pi}\frac{tan\beta}{sin^2\theta_W}\frac{m_\mu^2}{\tilde{m}_2\mu}[\frac{\mu^2}{\mu^2-\tilde{m}_2^2}F_1 - \frac{\tilde{m}_2^2}{\mu^2-\tilde{m}_2^2}F_2]$$

where $F_i = F(m_{\tilde{\nu}}^2/m_{\tilde{\chi}_i^2})$ are positive form factors from loop integrals and $\tilde{m}_2 \simeq 0.8 m_{1/2}$.

Note for characteristic parameters, $m_{1/2} = 480$ GeV, $\mu = 690$ GeV, $\tan\beta = 25$:

$$\frac{\alpha}{4\pi}\frac{tan\beta}{sin^2\theta_W}\frac{m_\mu^2}{\tilde{m}_2\mu} = 27\times 10^{-10}$$

in the experimental region of BNL data.

[The neutralino diagram is small due to special cancellations (next page).]

Neutralino contribution for large tanβ, small M_W^2/μ^2

$$a_\mu^{\tilde{\chi}^0} \simeq \frac{\alpha}{4\pi}\frac{tan\beta}{cos^2\theta_W}\frac{m_\mu^2}{\tilde{m}_2\mu}[(\frac{\mu^2}{m_{\tilde{\mu}_L}^2 - m_{\tilde{\mu}_R}^2} - \frac{\mu^2}{\mu^2 - \tilde{m}_1^2})G_{11}]$$

$$-(\frac{\mu^2}{m_{\tilde{\mu}_L}^2 - m_{\tilde{\mu}_R}^2} - \frac{1}{2}\frac{\mu^2}{\mu^2 - \tilde{m}_1^2})G_{21}$$

$$-\frac{1}{2}\frac{\tilde{m}_1}{\tilde{m}_2}\frac{1}{\tan\theta_W^2}\frac{\mu^2}{\mu^2 - \tilde{m}_2^2}G_{22}+$$

$$\frac{1}{4}\frac{\tilde{m}_1}{\mu}\frac{1}{\tan\theta_W^2}\frac{\mu^2}{\mu^2 - \tilde{m}_2^2}(1 + \frac{\tilde{m}_2}{\mu})G_{23}$$

where $c_W^2 = cos^2\theta_W$,$\tilde{m}_1 \simeq 0.4 m_{1/2}$ and $G_{kj} = G(m_{\chi_j^2/\tilde{\mu}_k^2) > 0}$.

For $m_{1/2} = 480$ GeV, $\mu = 690$ GeV, $\tan\beta = 25$:

$$\frac{\alpha}{4\pi}\frac{tan\beta}{cos^2\theta_W}\frac{m_\mu^2}{\tilde{m}_1\mu} = 16 \times 10^{-10}$$

but the 2nd term cancels $\sim$ 75% of the first term and the last two terms are small.

We have that the sign of a_μ is the sign of μ[Lopez, Nanopoulos, Wang(1994); Chattopadhyay, Nath(1996)] and since experiment indicates a positive anomaly:

$$\mu > 0$$

(i) Good news for dark matter detection for if $\mu < 0$, cancellations can occur reducing cross section to $\sigma_{\tilde{\chi}^0_1 - p} < 10^{-12}$ pb which would be unaccessible to all future planned detctions. [Fig. $\mu < 0$]

(ii) Good news for theory for if a_μ had implied $\mu < 0$, the $b \to s\gamma$ constraint would have eliminated almost all the parameter space.

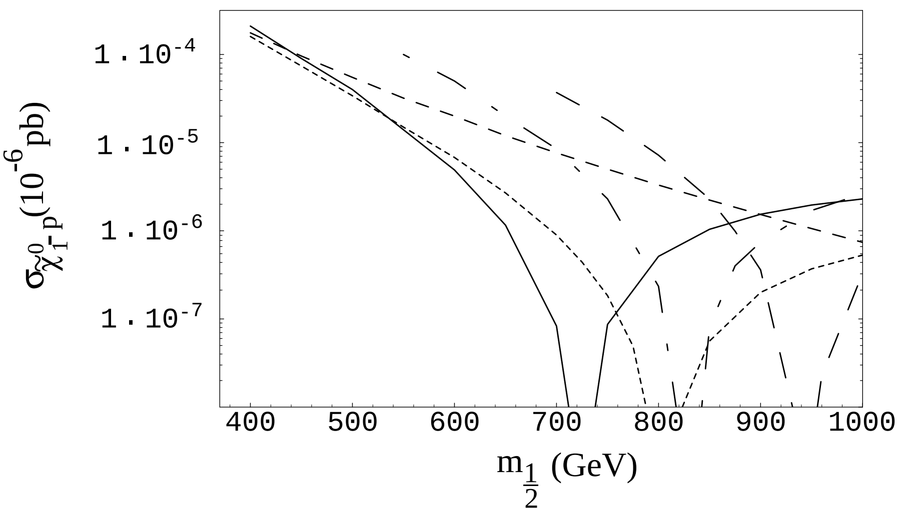

$\sigma_{\tilde{\chi}_1^0-p}$ for mSUGRA for $\mu < 0$, $A_0 = 1500$ GeV, for $\tan\beta = 6$ (short dash), $\tan\beta = 8$ (dotted), $\tan\beta = 10$ (solid), $\tan\beta = 20$ (dot-dash), $\tan\beta = 25$ (dashed). Note that the $\tan\beta = 6$ curve terminates at low $m_{1/2}$ due to the Higgs mass constraint, and the other curves terminate at low $m_{1/2}$ due to the $b \to s\gamma$ constraint.

Now accelerator constraints on m_h and $b \to s\gamma$ imply most of parameter space is in co-annihilation region. Here m_0 is essentially determined by $m_{1/2}$ (for fixed A_0, $\tan\beta$) and is an increasing function of $m_{1/2}$. [Fig. $m_0 - m_{1/2}$ corridors]

Further, a_μ^{SUGRA} decreases as $m_{1/2}$, m_0 increase.

Hence:
(i) Lower bound on a_μ^{SUGRA} determines upper bound on $m_{1/2}$.

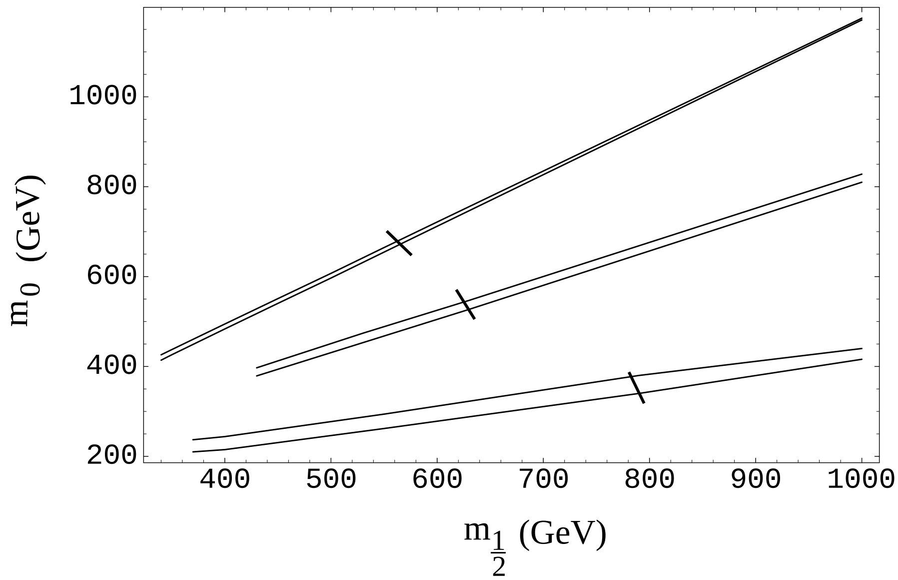

Corridors in the $m_0 - m_{1/2}$ plane allowed by the relic density constraint for $\tan\beta = 40$, $m_h > 111$ GeV, $\mu > 0$ for $A_0 = 0, -2m_{1/2}, 4m_{1/2}$ from bottom to top. The curves terminate at low $m_{1/2}$ due to the $b \to s\gamma$ constraint except for the $A_0 = 4m_{1/2}$ which terminates due to the m_h constraint. The short lines through the allowed corridors represent the high $m_{1/2}$ termination due to the lower bound on a_μ.

(ii) But also, m_h increases as $m_{1/2}$ and $\tan\beta$ increase, and since a_μ lower bound fixes an upper bound on $m_{1/2}$, a lower bound on m_h implies a lower bound on $\tan\beta$.

At 95% C.L. find

$m_h > 114$ GeV:

$\tan\beta > 7$; $A_0 = 0$
$\tan\beta > 5$; $A_0 = -4m_{1/2}$

$m_h > 120$ GeV:

$\tan\beta > 15$; $A_0 = 0$
$\tan\beta > 10$; $A_0 = -4m_{1/2}$

Thus the combined constraints of

m_h, a_μ^{SUGRA}, $b \to s\gamma$, relic density

have begun to strongly limit the parameter space and thus sharpen predictions:

(1) a_μ^{SUGRA}

Fig. $a_\mu^{\text{SUGRA}} - m_{1/2}$

One sees that mSUGRA can not accommodate large values of a_μ^{SUGRA} and if the final data gives an anomaly greater then $\simeq 50 \times 10^{-10}$, this would indicate breakdown of mSUGRA (posssible non-universal terms)

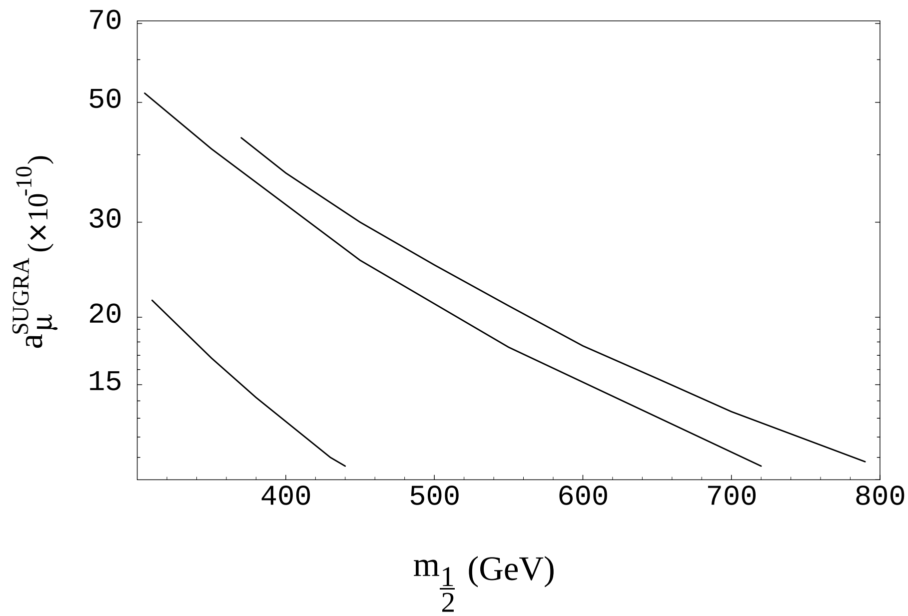

mSUGRA contribution to a_μ as a function of $m_{1/2}$ for $A_0 = 0$, $\mu > 0$, for $\tan\beta = 10$, 30 and 40 (bottom to top) and $m_h > 111$ GeV.

(2) Accelerator Physics

The restricted parameter space allows sharpening of predictions of SUSY mass spectrum at accelerators. Consider

$$a_\mu^{\mathrm{SUGRA}} > 21 \times 10^{-10};\ 90\% C.L.$$

For $A_0 = 0$ we have $\tan\beta > 10$ and $m_{1/2} = (290 - 550)$ GeV; $m_0 = (70 - 300)$GeV for $\tan\beta < 40$.

[Table-SUSY masses; 90% C.L.]

Accelerator reaches:

Tevatron RUN II: h (if $m_h \leq 130 GeV$)

No trilepton signal.

NLC (500 GeV): h, $\tilde{\tau}_1$ and $\tilde{e}_1$ (partial coverage)

LHC: All SUSY particles.

Table 1. Allowed ranges for SUSY masses in GeV for mSUGRA assuming 90% C. L. for a_μ for $A_0 = 0$. The lower value of $m_{\tilde{t}_1}$can be reduced to 240 GeV by changing A_0 to -4$m_{1/2}$. The other masses are not sensitive to A_0.

$\tilde{\chi}_1^0$	$\tilde{\chi}_1^\pm$	$\tilde{g}$	$\tilde{\tau}_1$
(123-237)	(230-451)	(740-1350)	(134-264)

$\tilde{e}_1$	$\tilde{u}_1$	$\tilde{t}_1$
(145-366)	(660-1220)	(500-940)

(3) Darkmatter ($\tilde{\chi}_1^0$) Detection

Governed by $\sigma_{\tilde{\chi}_1^0-p}$ which decreases with increasing m_o, $m_{1/2}$,. Since a_μ^{SUGRA} minimum has reduced upper bounds on $m_{1/2}$, this raises bounds on $\sigma_{\tilde{\chi}_1^0-p}$.

[Fig. $\sigma_{\tilde{\chi}_1^0-p}$, $\tan\beta = 40$, $\mu > 0$]
$\sigma_{\tilde{\chi}_1^0-p} > 6 \times 10^{-10}$ pb; $\tan\beta = 40$

Reducing $\tan\beta$ should make $\sigma_{\tilde{\chi}_1^0-p}$ smaller, However the a_μ bound then eliminates more of high m_0, $m_{1/2}$ compensating

[Fig. $\sigma_{\tilde{\chi}_1^0-p}$, $\tan\beta = 10$, $\mu > 0$]
$\sigma_{\tilde{\chi}_1^0-p} > 4 \times 10^{-10}$ pb; $\tan\beta = 10$

Almost all of mSUGRA parameter space should now be accessible to future dark matter detectors.

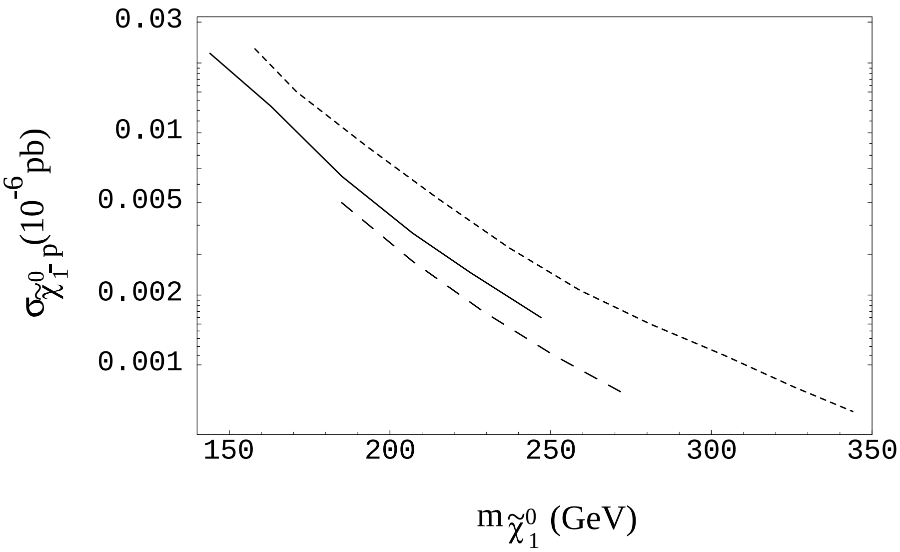

$\sigma_{\tilde{\chi}^0_1-p}$ as a function of the neutralino mass $m_{\tilde{\chi}^0_1}$ for $\tan\beta = 40$, $\mu > 0$ for $A_0 = -2m_{1/2}, 4m_{1/2}, 0$ from bottom to top. The curves terminate at small $m_{\tilde{\chi}^0_1}$ due to the $b \to s\gamma$ constraint for $A_0 = 0$ and $-2m_{1/2}$ and due to the Higgs mass bound ($m_h > 111$ GeV) for $A_0 = 4m_{1/2}$. The curves terminate at large $m_{\tilde{\chi}^0_1}$ due to the lower bound on a_μ.

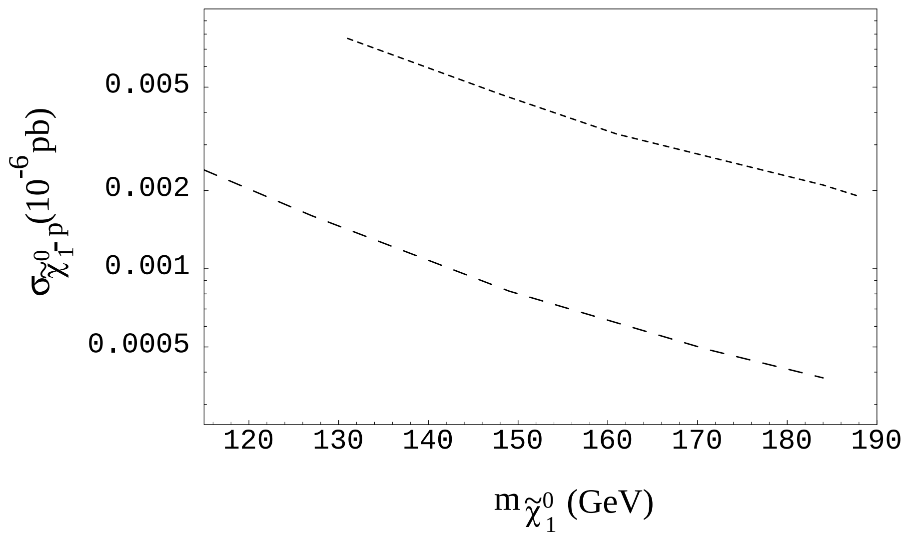

$\sigma_{\tilde{\chi}_1^0-p}$ as a function of $m_{\tilde{\chi}_1^0}$ for $\tan\beta = 10$, $\mu > 0$, $m_h > 111$ GeV for $A_0 = 0$ (upper curve), $A_0 = -4m_{1/2}$ (lower curve). The termination at low $m_{\tilde{\chi}_1^0}$ is due to the m_h bound for $A_0 = 0$, and the $b \to s\gamma$ bound for $A_0 = -4m_{1/2}$. The termination at high $m_{\tilde{\chi}_1^0}$ is due to the lower bound on a_μ.

5. NON-UNIVERSAL MODELS

Parameterize non-universal Higgs and 3rd generation soft breaking masses:

$$m_{H_1}^2 = m_0^2(1 + \delta_1); \quad m_{H_2}^2 = m_0^2(1 + \delta_2);$$

$$m_{q_L}^2 = m_0^2(1 + \delta_3); \quad m_{t_R}^2 = m_0^2(1 + \delta_4);$$

$$m_{\tau_R}^2 = m_0^2(1 + \delta_5);$$

$$m_{b_R}^2 = m_0^2(1 + \delta_6); \quad m_{l_L}^2 = m_0^2(1 + \delta_7).$$

with

$$-1 < \delta_i < +1$$

μ^2 governs much of the physics ($t \equiv \tan\beta$):

$$\mu^2 = \frac{t^2}{t^2-1}\Big[(\frac{1-3D_0}{2}+\frac{1}{t^2})+$$

$$\frac{1-D_0}{2}(\delta_3+\delta_4)-\frac{1+D_0}{2}\delta_2+\frac{\delta_1}{t^2}\Big]\, m_0^2+$$

universal parts + loop corrections.

where D_0 is small i.e. $D_0 \simeq 0.25$. Universal m_0 part not large, and so μ^2 can be raised or lowered by δ_i corrections.

Most interesting new effects occur if μ^2 is lowered for then
(i) Open new $\tilde{\chi}^0_1$ annihilation channel through s-channel Z^0-pole.

(ii) Lowering μ^2 increases $\sigma_{\tilde{\chi}^0_1-p}$

(1) δ_2=1; all other δ_i=0
[Fig: Allowed $m_0 - m_{1/2}$ region for $\delta_2 = 1$]
[Fig: $\sigma_{\tilde{\chi}^0_1-p}$ for δ_2=1]
We see Z-channel gives large $\sigma_{\tilde{\chi}^0_1-p}$, testable for CDMS in Soudan mine.

(2) $\delta_{10}(=\delta_3=\delta_4=\delta_5)=-0.7$

The $\tilde{\tau}_1 - \tilde{\chi}^0_1$ corridor moved up in m_0 [Fig. allowed $\sigma_{\tilde{\chi}^0_1-p}$ for $\delta_{10} = -0.7$] Again Z-channel gives rise to large cross sections.

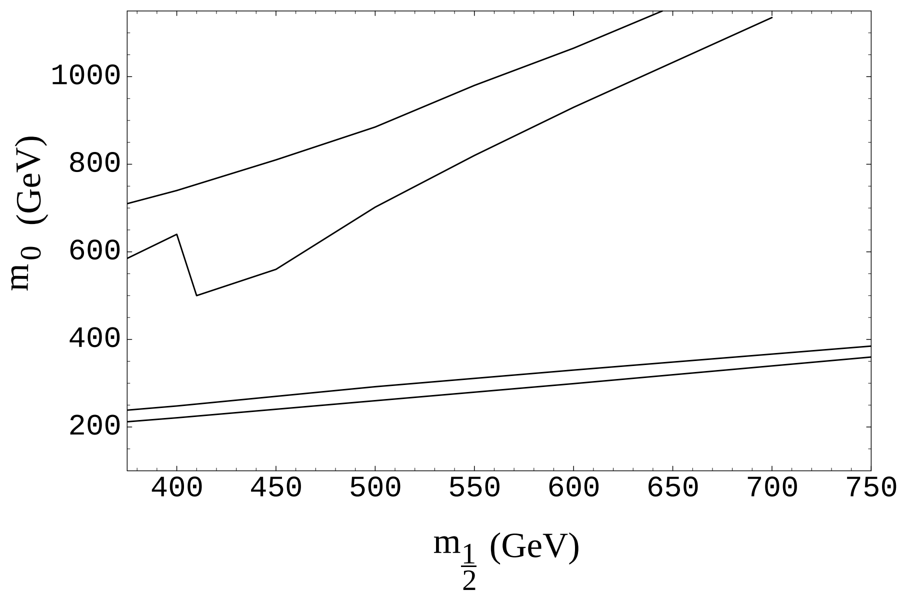

Effect of a nonuniversal Higgs soft breaking mass enhancing the Z^0 s-channel pole contribution in the early universe annihilation, for the case of δ_2 =1, $\tan\beta = 40$, $A_0 = m_{1/2}$, $\mu > 0$. The lower band is the usual $\tilde{\tau}_1$ coannihilation region. The upper band is an additional region satisfying the relic density constraint arising from increased annihilation via the Z^0 pole due to the decrease in μ^2 increasing the higgsino content of the neutralino.

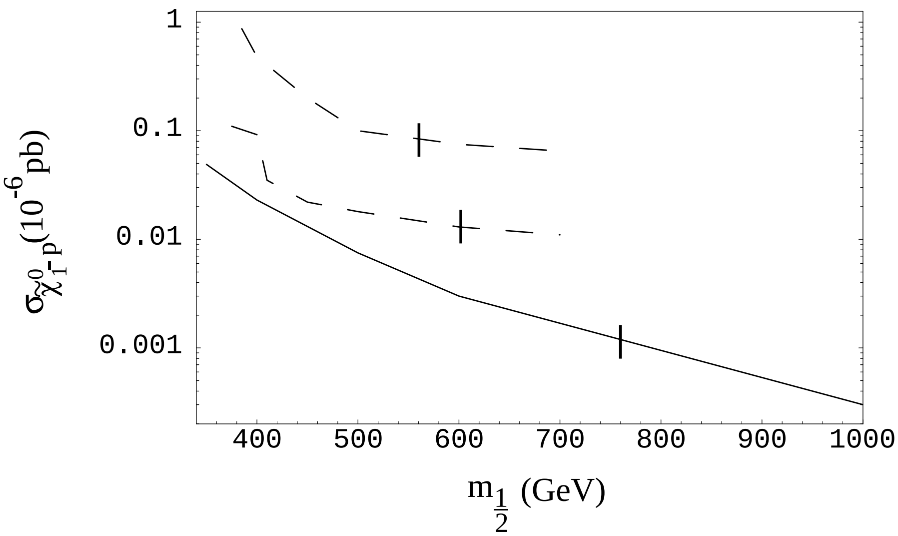

$\sigma_{\tilde{\chi}^0_1 - p}$ as a function of $m_{1/2}$ ($m_{\tilde{\chi}^0_1} \cong 0.4 m_{1/2}$) for $\tan\beta = 40$, $\mu > 0$, $m_h > 111$ GeV, $A_0 = m_{1/2}$ for $\delta_2 = 1$. The lower curve is for the $\tilde{\tau}_1 - \tilde{\chi}^0_1$ co-annihilation channel, and the dashed band is for the Z s-channel annihilation allowed by non-universal soft breaking. The curves terminate at low $m_{1/2}$ due to the $b \to s\gamma$ constraint. The vertical lines show the termination at high $m_{1/2}$ due to the lower bound on a_μ.

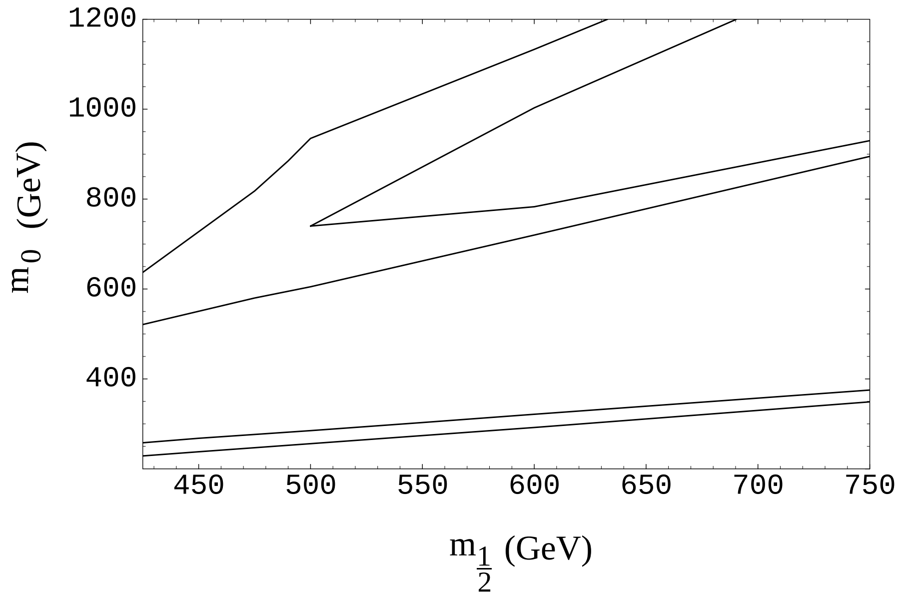

Allowed regions in the $m_0 - m_{1/2}$ plane for the case $\tan\beta = 40$, $A_0 = m_{1/2}$, $\mu > 0$. The bottom curve is the mSUGRA $\tilde{\tau}_1$ coannihilation band of (shown for reference). The middle band is the actual $\tilde{\tau}_1$ coannihilation band when $\delta_{10} = -0.7$. The top band is an additional allowed region due to the enhancement of the Z^0 s-channel annihilation arising from the nonuniversality lowering the value of μ^2 and hence raising the higgsino content of the neutralino. For $m_{1/2} \lesssim 500$ GeV, the two bands overlap.

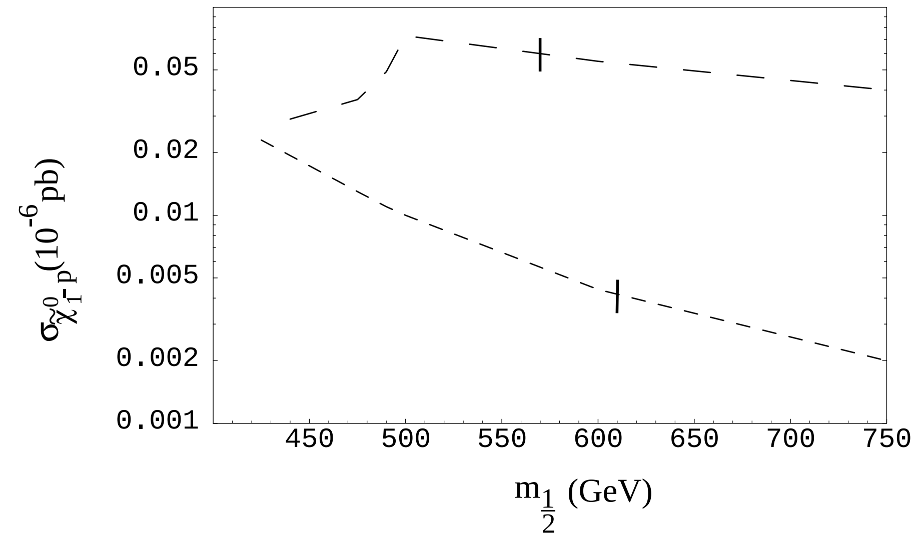

$\sigma_{\tilde{\chi}_1^0-p}$ as a function of $m_{1/2}$ for $\delta_{10} = -0.7$ for $\tan\beta = 40$, $\mu > 0$, $A_0 = m_{1/2}$ and $m_h > 111$ GeV. The lower curve is for the bottom of the $\tilde{\tau}_1 - \tilde{\chi}_1^0$ co-annihilation corridor, and the upper curve is for the top of the Z channel band. The termination at low $m_{1/2}$ is due to the $b \to s\gamma$ constraint, and the vertical lines are the upper bound on $m_{1/2}$ due to the lower bound of a_μ.

6. CONCLUSIONS

We have examined the 2.6σ deviation of a_μ from the Standard Model within the framework of SUGRA model with R-parity invariance.

The combined experimental constraints from a_μ, m_h, $b \to s\gamma$, and darkmatter ($\tilde{\chi}_1^0$) relic density interact strongly and allow one to greatly sharpen theoretical predictions.

For mSUGRA:
(i) Lower bound of a_μ implies $m_{1/2} < 550(790)$ at 90%(95%) C.L.; $\tan\beta < 40$

(ii) $m_h > 114$ GeV: $\tan\beta > 7(5)$ for $A_0 = 0(-4m_{1/2})$
$m_h > 120$ GeV: $\tan\beta > 15(10)$ for $A_0 = 0(-4m_{1/2})$

(iii) Accelerator reach (90% C.L.) :
Tevatron RUN II: h (for $m_h < 130$ GeV)
NLC (500 GeV):$\tilde{\tau}_1$, h, $\tilde{e}_1$ (part of parameter space)
LHC: All SUSY particles.

(iv) Future planned dark matter detectors should be able to sample almost all of SUSY parameter space.

(v) mSUGRA implies $a_\mu^{\mathrm{SUGRA}} \leq 50 \times 10^{-10}$; for $\tan\beta \leq 40$.

Non-universal SUGRA models allow new regions of parameter space (early universe annihilation of $\tilde{\chi}_1^0$ through s-channel Z-poles) leading to $\sigma_{\tilde{\chi}_1^0 - p}$ accessible to current darkmatter detectors.

Further BNL a_μ data should reduce current errors, allowing more precise predictions of SUGRA model.